applied sciences

MDPI

Article

Induction of Highly Dynamic Shock Waves in Machining Processes with Multiple Loads and Short Tool Impacts

Andreas Tausendfreund [1,*], Dirk Stöbener [1,2] and Andreas Fischer [1,2]

[1] University of Bremen, Bremen Institute for Metrology, Automation and Quality Science (BIMAQ), Linzer Straße 13, 28359 Bremen, Germany; std@bimaq.de (D.S.); fischer@bimaq.de (A.F.)
[2] MAPEX Centre for Materials and Processes, University of Bremen, 28359 Bremen, Germany
* Correspondence: a.tausendfreund@bimaq.de; Tel.: +49-421-218-64641

Received: 15 April 2019; Accepted: 30 May 2019; Published: 4 June 2019

Abstract: In order to study the mechanical loads of a workpiece in manufacturing processes such as single-tooth milling, in-process measurements of workpiece deformations are required. To enable the resolution of shock waves due to the mechanical impact of the tool, a novel measurement system based on speckle photography is introduced to measure the dynamic deformations and strains with a high temporal and spatial resolution. The measurement results indicate deformations and strains propagating through the workpiece with the speed of sound triggered by the tool impact (i.e., the tool impact is shown to induce shock waves during milling). Finite element simulations of the workpiece behavior are performed in addition, which support the experimental findings. In the considered case, the dynamic excitation subsides after 300 ms. Hence, in processes with even shorter cyclic multiple loads, the tool encounters an already excited initial state during machining, which needs to be taken into account when precisely modeling the milling process and the resulting workpiece quality. Finally, the measurement results demonstrate that speckle photography in combination with modern high-speed cameras and compact short-pulse lasers provides a deeper understanding of individual manufacturing processes.

Keywords: speckle photography; process dynamics; single-tooth milling; chip formation; finite element method simulation

1. Introduction

Current research work aims to describe production steps independently of the process using the so-called process signature, which summarizes all interactions between material and process [1,2]. This new way of looking at and describing should enable the processing of materials in an even more targeted way, so that they can be optimally adapted to the respective requirements. The basic prerequisite for this is an exact understanding of the individual manufacturing processes. In this context, the cutting process with a defined cutting edge, as it occurs during turning and milling, is considered in this article. In order to understand chip formation and chip breakage, it is particularly important to determine the relationship between the loads acting on the material during machining and the changes remaining in the material afterwards.

The loads in terms of the strains can be quantified during the production process by means of speckle photography [3,4]. With this method, the surface to be measured is illuminated with a laser and the evaluation areas in the speckle images taken with the camera—before and during the occurrence of the deformation—are correlated with each other [5,6]. From the correlated image sections, local displacements can be calculated, whose theoretical resolutions are limited only by Heisenberg's uncertainty relation [7]. Due to the availability of compact diode lasers with a short-pulse length of

less than 1 ns and pulse energies of more than 20 µJ, it is possible to integrate the measuring system into the machining area of machine tools and to investigate dynamic manufacturing processes with tool speeds of, for instance, more than $v_c = 10 \frac{m}{s}$ [8].

However, the measuring of the remaining modifications (plastic deformations), which are ten times weaker in relation to the loads (elastic + plastic deformations), has been proven difficult so far, especially in processes with multiple stresses due to recurring loads and cyclic machining processes (e.g., milling). The modifications remaining in the material surface layer after the last tool intervention are usually inhomogeneous [8]. In extreme cases, the periodic fluctuations of the modification also occur under continuous cutting conditions (as in the turning process) and correlate with undesired chatter marks on the surface, which can be seen in Figure 1.

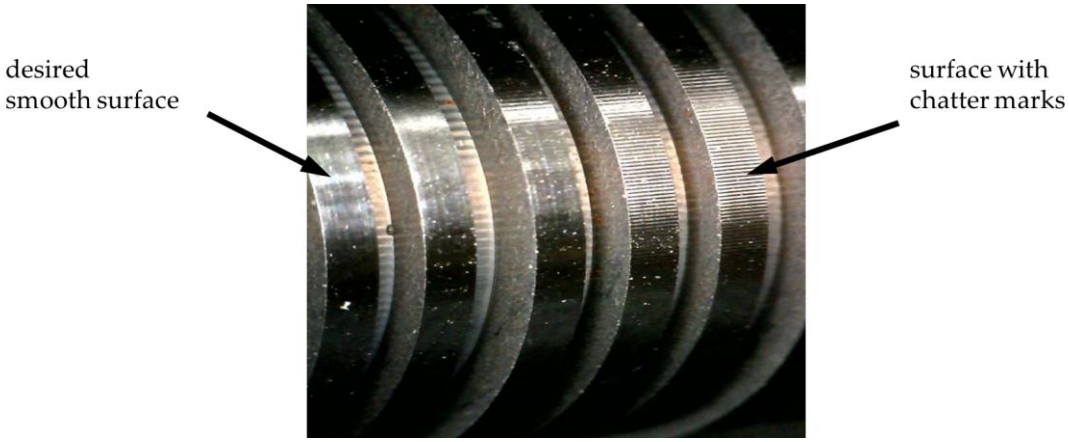

Figure 1. Undesired chatter marks in a turning process (right half of picture).

The properties of the chatter marks, such as periodicity and amplitude, are influenced by the resonance behavior of the complex manufacturing system [9]. A causal trigger in the continuous process can be the disturbance of the system due to the effect of chip breakage or chip formation depending on the workpiece condition [10]. The chip formation and chip breakage were investigated theoretically by means of finite element method (FEM) simulations, compared with high speed videos and discussed with the relationship to the process stability and the surface quality produced [11].

When researching chip separation and chatter mark formation, mainly the resonance and vibration behavior of the machine tool and the workpiece are considered. Induced workpiece vibrations and dynamic strain states are difficult to determine so far, therefore these effects are currently not included in the investigations. In this respect, it is also not known how the remaining modifications in the form of periodic fluctuations of the strain [8] are related to chip formation or chip breakage. However, it is probable that both the chip breakage and the penetration of the tool at the beginning of the chip formation generate a shock wave, which propagates through the material at the speed of sound. The open scientific questions therefore are:

- Are dynamic processes in the workpiece stimulated during machining and is the lifetime of these shock waves long enough to cause feedback in processes with multiple loads (such as milling)?
- Can the excited workpiece states be measured with the aid of speckle photography?

The aim of the paper is to investigate whether and how the external mechanical excitations of the workpiece affect internal mechanical properties such as deformation or strain, and to investigate these properties both theoretically and experimentally. For this purpose, after a short introduction to the theory of speckle photography (Section 2.1) and the presentation of the measurement setup (Section 2.2), measurements are carried out in a running single-tooth circumferential milling process with a rotating tool (Section 3.1). These measurements are then compared with FEM simulations of a linear cutting process with constant cutting conditions and defined cutting edge (Section 3.2). In order

to enable a validation of the measuring method by the simulation results, the feed rate in the real milling process was selected in such a way that almost constant cutting conditions prevail here as well. The investigations of the resulting workpiece state due to multiple stresses are carried out in Section 3.3. For this purpose, the workpiece condition is examined by means of speckle photography, at the time when the tool would interact with the workpiece a second time after the first intervention. For the first time, shock waves induced by the tool impact could be measured using speckle photography. A comparison with theoretical investigations of the chip rupture and the resulting induced formation of strain waves propagating through the workpiece take place in Section 3.4. After a discussion of the results in Section 4, a conclusion is finally drawn in Section 5.

2. Materials and Methods

2.1. Measuring Principle and Measuring Setup of Speckle Photography

When a rough surface is illuminated with coherent laser light, bright and dark areas appear in the image plane of the camera, caused by constructive and destructive interference. According to surface statistics, these form a dot or so-called subjective speckle pattern. In a typical imaging system, many scattering waves with very different phases participate in the scattering process. This usually results in a very fine pattern with speckle diameters smaller than the pixel size of the camera chip. If the light path is restricted by inserting an aperture, the size of the speckle can be adjusted as desired (see Figure 2).

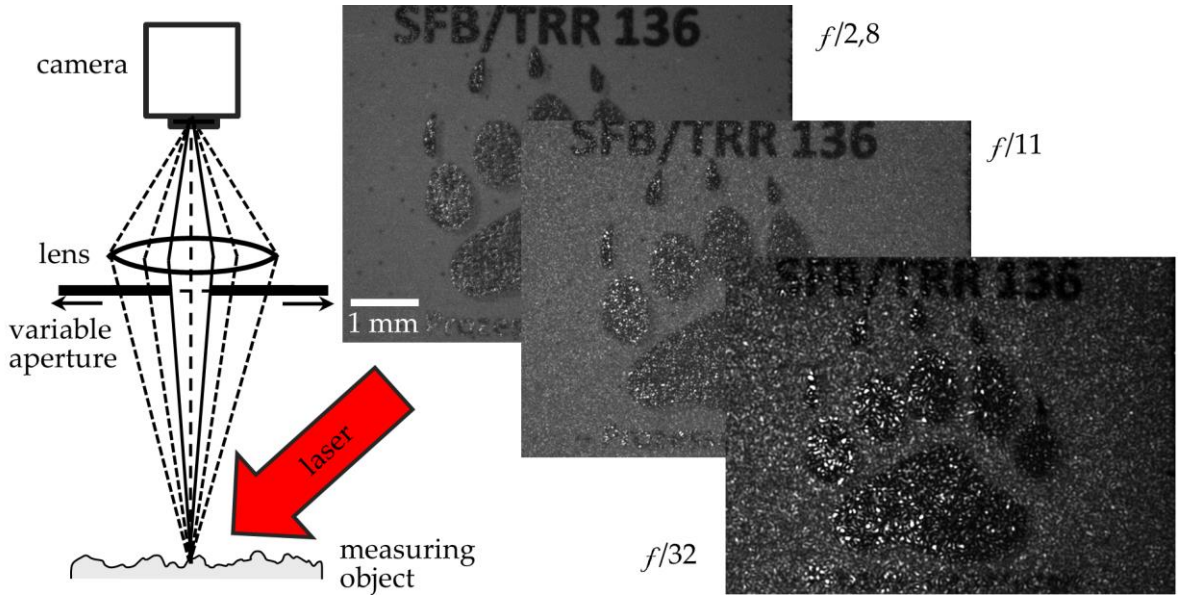

Figure 2. Image of the printed logo of the Transregional Collaborative Research Center and the behavior of the subjective speckle pattern when decreasing the aperture (increasing the f-number).

An outstanding characteristic of subjective speckles is that they are assigned to specific surface points according to the imaging system. To calculate surface displacements, a small evaluation window scans across the non-deformed (time t_n) and the deformed speckle image (time t_{n+1}) and calculates the cross correlation between the states at both time points at each evaluation position. The size of the evaluation window can be calculated automatically and should contain at least three speckles on the diagonal. According to Zhou and Goodson, a speckle diameter of 3–5 pixels should be used for the optimum size of the speckle to be set [12]. Deformation fields for surface deformations in the object plane (in-plane) with a measurement uncertainty of less than 22 nm can be determined from the displacement of the correlation maxima [8]. After the calculation of the deformation fields, the corresponding strain fields can be quantified via gradient formation according to Kajberg [13].

In practical terms, the measuring system is integrated into the production machine (Precitech Freeform 3000, Precitech, Inc., Keene, USA) in such a way that measurements can be taken on the front face of the workpiece (42CrMo4) (see Figure 3a).

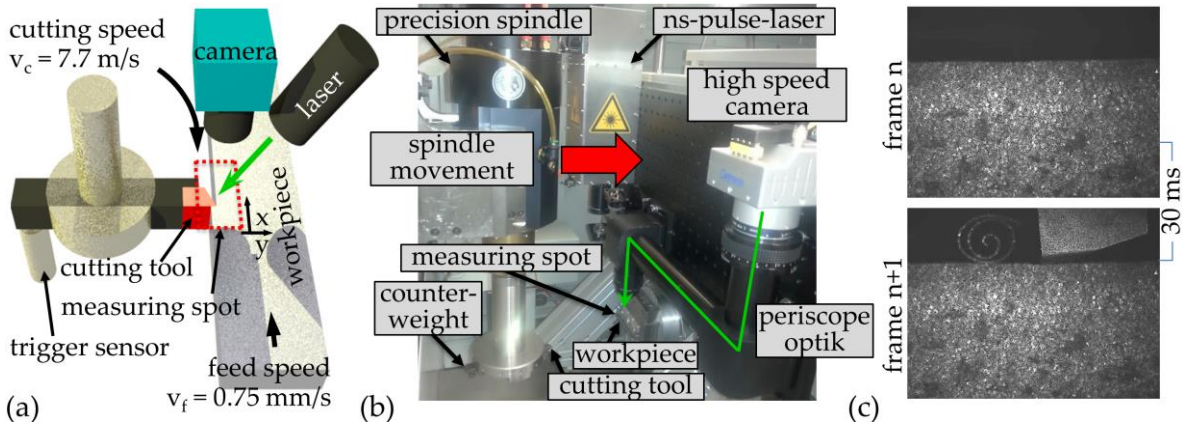

Figure 3. Use of speckle photography for single-tooth circumferential milling: (**a**) basic measurement setup, (**b**) integration into the processing machine, and (**c**) camera shots of the unloaded and loaded condition.

Since the spindle of the tool is located above the workpiece, it occupies the possible mounting space for the camera so that the required field of view cannot be observed directly. Therefore, a special periscope lens had to be developed for the camera (Figure 3b). In order to ensure a constant position of the workpiece during image acquisition, trigger marks are attached to both the tool holder and the counterweight. Triggered images can thus be taken when the tool is engaged and when it is replaced by the counterweight (Figure 3c). Compared to the conventional turning process [14], the cutting conditions were set slightly higher with a cutting speed of $v_c = 7.7\ \frac{m}{s}$, a cutting depth of $a_p = 0.5$ mm, and a feed speed of $v_f = 0.75\ \frac{mm}{s}$ in order to test the resolution limits with respect to the measuring speed of the measuring system. The corresponding cutting geometry is illustrated in Figure 4.

To enable in-process measurements with displacement resolutions in the small two-digit nanometer range at the high cutting speeds, it is necessary that the object to be measured moves by a maximum of ten nanometers during camera exposure. This is achieved by using a short-pulse laser with a pulse length of less than one nanosecond. Both on the forming chip and on the rotating tool a non-smeared speckle pattern suitable for evaluation can be observed (see Figure 3c) even in dynamic production processes with tool speeds of up to $v_c = 7.7\ \frac{m}{s}$.

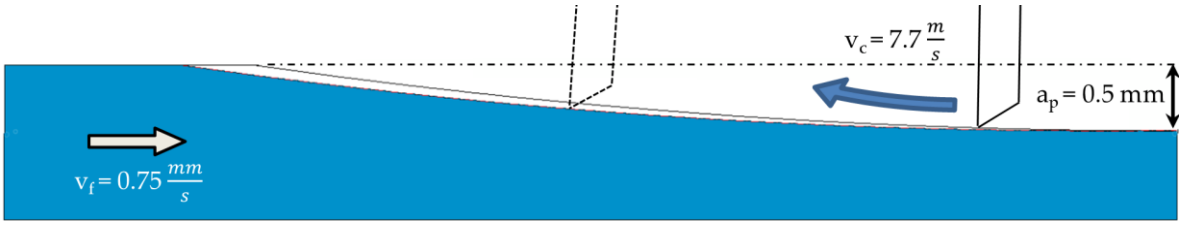

Figure 4. Cutting geometry for single-tooth circumferential milling.

2.2. FEM Simulation and Setup of Simulation

The theoretical investigation of chip formation, chip separation, and the possibly developing shock wave is carried out with a 2D FEM simulation of the flat strain state. The measuring setup shown in Figure 3 with a rotating tool is approximated by a linear tool movement in the x-direction. This is possible due to the large radius of the milling cutter (150 mm) in relation to the low cutting depth (50–500 µm). Despite the rotating tool and the slowly changing chip thickness, the cutting conditions

in the milling process are almost constant at a first approximation. The tool impact can also cause dynamic excitation of the workpiece. However, the cutting edge slowly plunges into the workpiece due to the movement on a circular path (see Figure 4). In order to keep the simulation as simple as possible, the mechanical load during penetration of the milling tool is not considered.

Figure 5 illustrates the geometry model for the FEM simulation. The material used for the workpiece is structural steel with a modulus of elasticity of 2×10^{11} Pa and a maximum tensile strength of 4.6 x 10^8 Pa. With a cutting speed $v_c = 7.7 \frac{m}{s}$ and a cutting depth a_p = 500 µm, the applied cutting conditions are identical to those of the measured milling process. The workpiece size (30 x 15 mm) was also adapted to the measured process; the minimum mesh distance at the region of interest is 45 µm. In the machine tool, the workpiece is magnetically clamped to the base surface, therefore the base surface is considered static in the simulation.

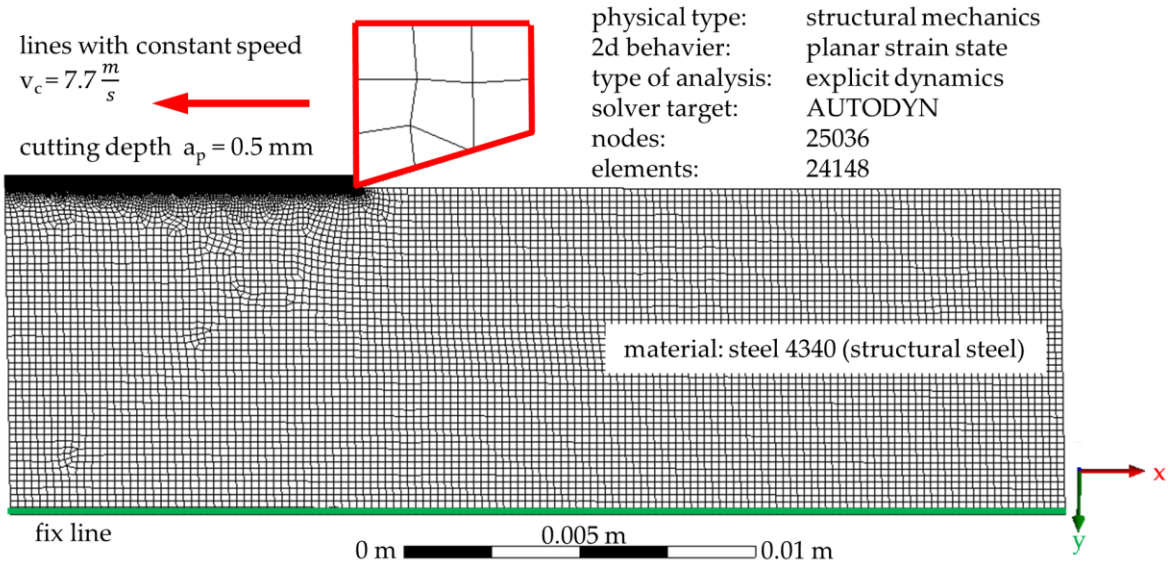

Figure 5. Geometry model of the milling process for finite element method (FEM) simulation.

3. Results

3.1. Measured Material Loads and Modifications

Figure 6 shows the loads for the single-tooth milling process, measured during tool engagement using speckle photography. Since the cutting depth is smaller at the beginning of the tool engagement, a small impact results when the tool plunges into the workpiece. Due to a dynamic elastic out-of-plane movement of the workpiece in the edge area of the machined surface, this area (800 µm) cannot be included in the speckle correlation and is therefore not considered. The calculated deformation field for the x-direction in Figure 6a shows how the material on the workpiece surface is pushed in the negative x-direction. Maximum displacements of up to 1.8 µm are measured. Deformations in the y-direction occur mainly in the area in front of the cutting edge of the tool, whereby the deformations on the surface shown in Figure 6b are greatest with a maximum of 2 µm.

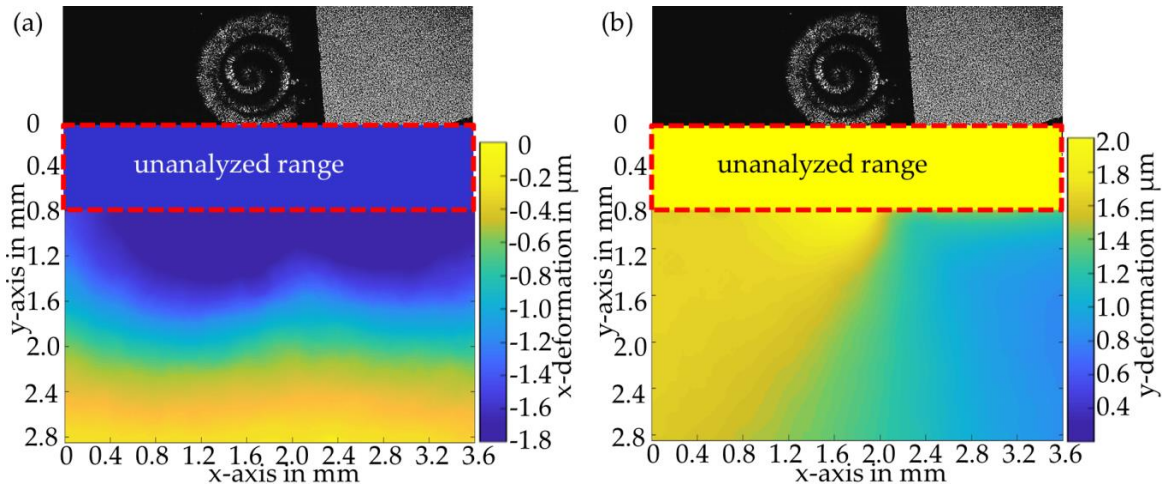

Figure 6. Loads measured by speckle photography during single-tooth milling. (**a**) Deformation in the x-direction and (**b**) deformation in the y-direction. The upper black and white area shows exemplarily the tool position and the chip formed in front of it.

The material modification remaining in the workpiece is determined by taking a speckle image in sufficient time after the last cut of the tool and comparing it with the image of the unloaded initial state. The evaluated displacement fields are shown in Figure 7.

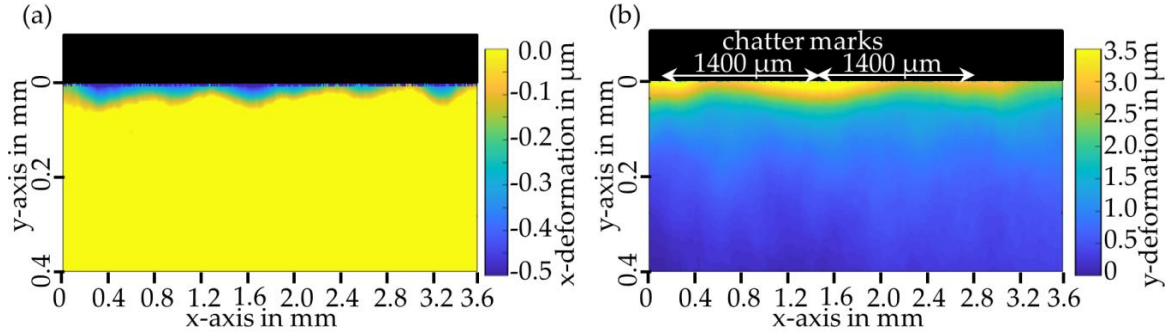

Figure 7. Remaining modification measured by speckle photography in the form of deformations: (**a**) x-deformation and (**b**) y-deformation.

On the one hand, it is noticeable that the remaining modifications in the form of displacements amount to only one tenth of the maximum displacement during load. Furthermore, it can be seen that the modifications are only limited to the upper 30–70 µm. In contrast to the dynamic load measurement, here the boundary to the machined surface can be evaluated much better when determining the remaining material modification. However, the evaluation of the displacements results in an increased measurement uncertainty in the edge area down to a depth of 150 µm compared to the mean uncertainty of 20 nm. The increased measurement uncertainty in the edge area is caused by the formation of a slight burr, corresponding to small plastic out-of-plane deformations of the measured front surface and filtering at the edge [8]. It is noticeable, however, that the periodic fluctuations coincide with the period of the chatter marks measured with a phase-contrast microscope in Figure 8. The measured modifications thus describe real machining effects despite the higher measurement uncertainty in the marginal area.

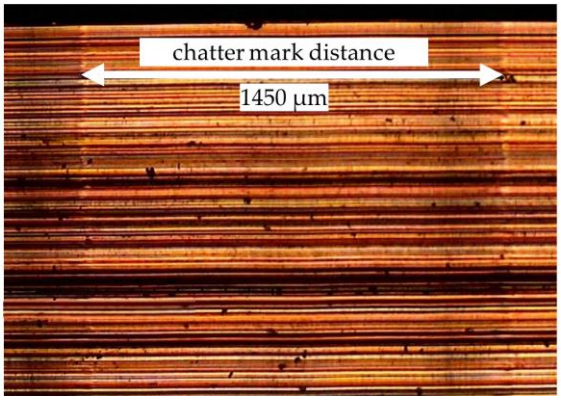

Figure 8. Chatter marks on machined workpiece surface, measured with a phase-contrast microscope.

3.2. Simulated Material Loads and Modifications

The validation of the measurement data is carried out with the help of FEM simulations. The cutting conditions in the simulation were chosen in such a way that the cutting forces in simulation and measurement match as closely as possible. The calculated displacements can be seen in Figure 9.

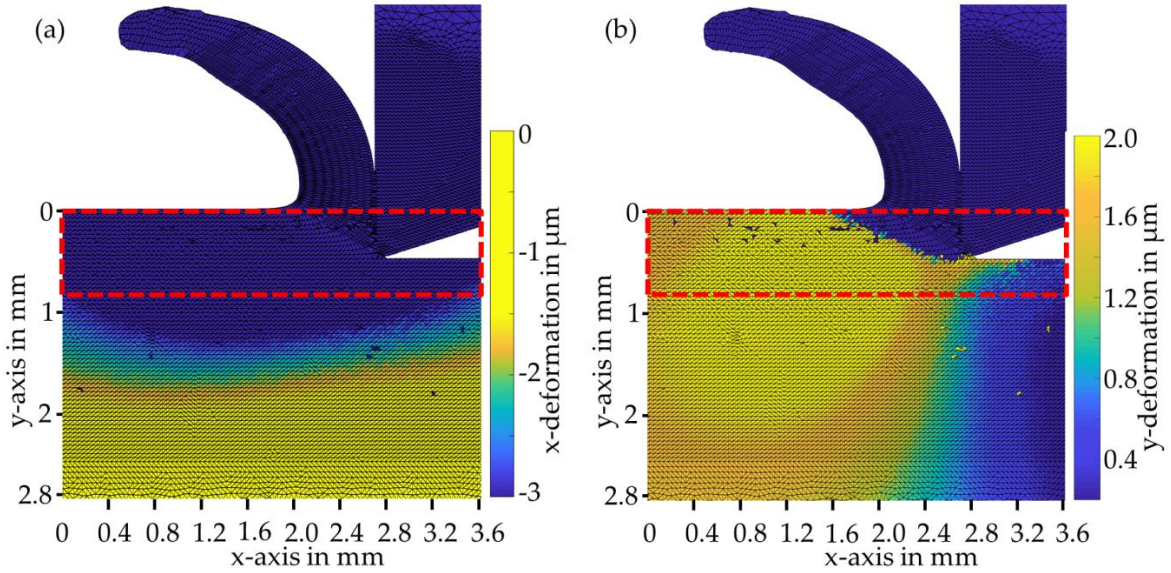

Figure 9. Simulated loads of single-tooth milling process. (**a**) Deformation in the x-direction and (**b**) deformation in the y-direction.

The measured (Figure 6b) and simulated (Figure 9b) y-displacement are almost identical, both in the penetration depth and in their maximum value of 2 µm. The penetration depths of the x-displacement in Figures 6a and 9a also agree well, but in terms of displacement the simulation results with a maximum of 3 µm are slightly larger than the value of 1.8 µm measured with speckle photography. One possible reason for the lower deformation may be the asymmetrical rigidity of the machine tool or tool holder. In the radial direction (y-direction), the stiffness of the tool holder is larger because only compressive forces act on the holder. A force in the x-direction, on the other hand, leads to a bending of the tool holder, which is approx. 20 mm long (black part in Figure 3a, shown here strongly shortened). A slow increase of the chip thickness along the cutting path leads to an increased bending of the tool holder during the cut. Therefore, the deformation of the workpiece in the x-direction is lower in the real process.

The simulated modifications remaining in the material after cutting are shown in Figure 10. The deformations in the y-direction (Figure 10b) vanished after cutting. Strong deformations remain

only on the left edge of the workpiece. They do not occur in the real process because there is no open interface and the tool leaves the workpiece with an upward direction component (see also cutting geometry in Figure 4). However, the displacements in the x-direction are obviously retained. In the upper right edge of the image (Figure 10a) the remaining deformations extend to a depth of 200 µm.

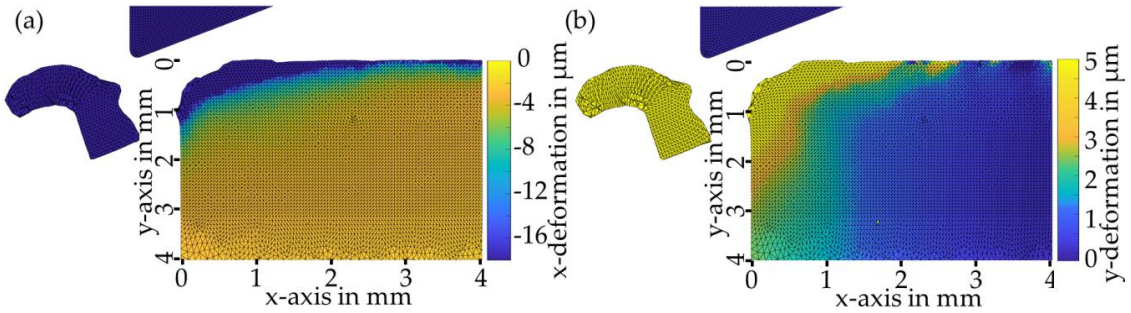

Figure 10. Simulated remaining modifications in the form of deformations: (**a**) x-deformation and (**b**) y-deformation.

As already mentioned in Section 3.1, it is assumed that the correlation algorithm of the evaluation generates increased measurement uncertainties in the marginal area of the surface, in particular due to the filtering at the edge. A quantitative comparison with the measurements is therefore not meaningful in this upper limit range. However, it should be noted that a very good quantitative agreement was also found at least for the measured loads in Figures 6 and 9.

3.3. Investigations of Multiple Stresses by Speckle Photography

In order to investigate the effects of multiple stresses in a manufacturing process with periodically recurring mechanical impact, speckle photography measurements were made after the last tool intervention. After the last cut, the tool slowly moved out of the workpiece in the -y-direction (see upper black and white area of each subimage of the picture sequence in Figure 11). The dynamic changes of the measured strains in the y-direction calculated from the speckle patterns are shown in the lower parts of the subimages in Figure 11. The dynamic excitation of the workpiece is conspicuous in this consideration of multiple loads. Only after approximately 300 ms a stable, final state results in relation to the unloaded case before the last tool impact. This means that in the subsequent cuts before, the tool always encounters a dynamically excited system, which must be taken into account when determining loads in this process with periodically recurring tool intervention. Note that due to the already excited system state, the strain measurement after 300 ms does not describe the overall remaining modification, but merely reflects the difference to the dynamic strain inherent to the state before the last tool impact. For an evaluation of the temporal course of multiple loads, it is therefore necessary to measure an image sequence that is as continuous as possible instead of individual snapshots, whereby the acquisition rates must correspond to the process dynamics. The required temporal resolution is estimated on the basis of the FEM simulation of the following section.

All in all, the speckle photographic measurements show that it is possible to describe the dynamic processes in the workpiece with sufficient spatial and displacement resolution by means of short-pulse exposure.

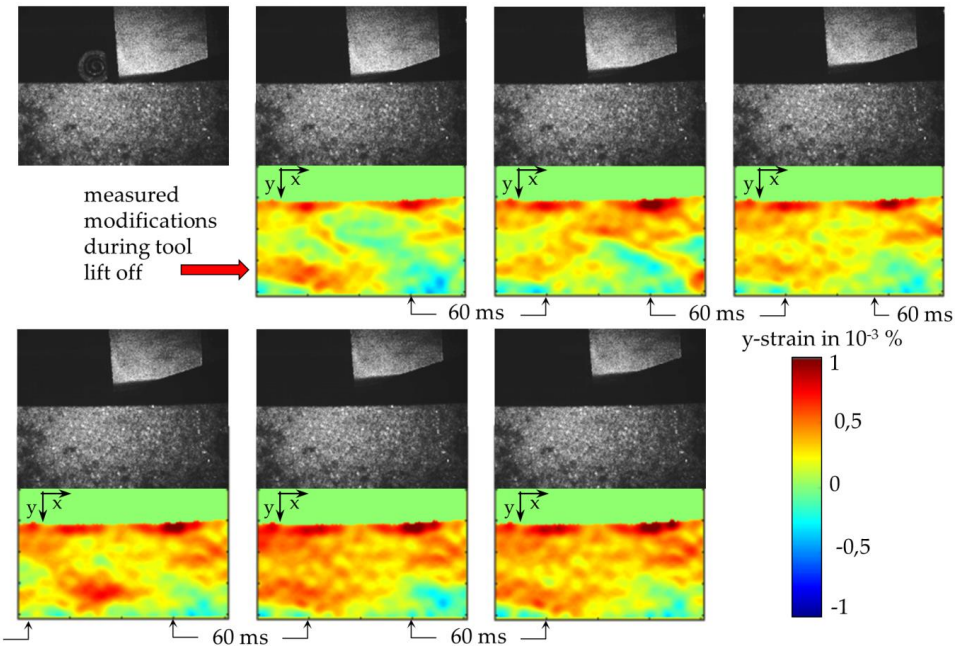

Figure 11. Image of the tool and the workpiece as well as the corresponding dynamic strain result after the last tool impact.

3.4. FEM Simulation of Shock Waves Occurring after Tool Engagement and Chip Breakage

In order to investigate the causes of the dynamic excitations and workpiece deformations, FEM simulations with high temporal resolution were carried out for the process of chip separation. In particular, the temporal change of the strain fields in the y-direction was examined, which is shown in Figure 12. It can be observed that expansion waves are released from the left side of the workpiece over a longer period of time, propagating in the direction of the upper right side of the workpiece (maximum drawn as black and white dashed lines). The maximum strain values of these shock waves are clearly above the values of the measured strains in Figure 11. This is due to the fact that a significantly longer time span (60 ms) has elapsed in the measurement in contrast to the time step in the simulation (0.5 µs).

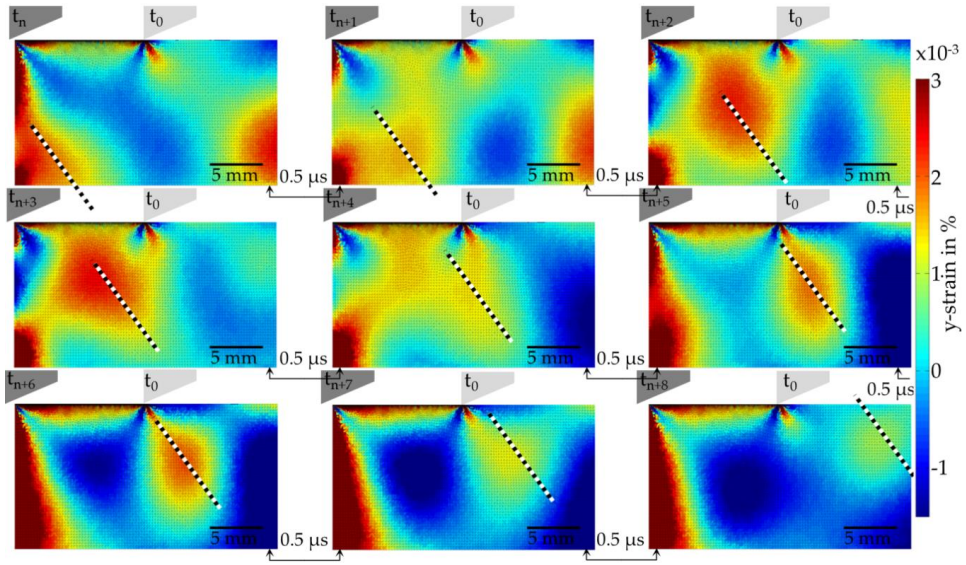

Figure 12. FEM simulation of shock waves after chip breakage for different time steps. The black and white dotted line is located on the maximum of the strain releasing from the lower left and symbolizes the strain front propagating through the material.

The calculation of the propagation velocity of the shock wave is done in Figure 13. For this purpose, the maximum in the area of the shock wave (black/white dashed line) is evaluated and the amount of the displacement vector is added to the last time step. The shock wave speed c_S results from the gradient in the plotted path-time diagram and is $c_S = 3318 \pm 452 \frac{m}{s}$. According to Rose [15], the sound velocities in structural steel are 5850 $\frac{m}{s}$ in the longitudinal direction and 3230 $\frac{m}{s}$ in the transverse direction. The propagation velocity of the simulated strain front thus corresponds within the uncertainty with the transverse propagation velocity of a sound wave in structural steel.

In the last time step of the simulation (Figure 12, bottom right) it can be seen that the observed shock wave runs to the top right against the edge of the workpiece. From this boundary surface, the wave is likely to be reflected back and forth in the workpiece until it is completely damped.

This explains why dynamic movements of the strain fronts are maintained over longer periods of time and can still be detected by speckle photography 300 ms after the last tool impact.

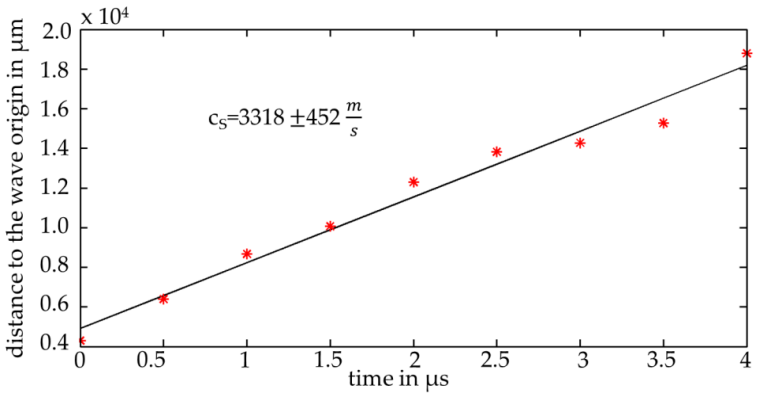

Figure 13. Velocity of propagation of the strain front, calculated from the displacement of the strain maximum (black and white dashed lines in Figure 12).

4. Discussion

In a single-tooth milling process, dynamic loads and modifications in the form of deformations and strains were measured using speckle photography. The validation approach of the in-process measurements for the highly dynamic manufacturing process of single-tooth circumferential milling was based on FEM simulations. For this, similar cutting conditions were used in the simulation as in the real manufacturing and measuring processes. The measured loads in the form of deformations agree qualitatively with the simulated results. In particular, the displacements in the y-direction are quantitatively equivalent, with a penetration depth of about 3 mm and a maximum displacement of 2 µm. Hence, the applicability of speckle photography for in-process measurements during a milling process is validated.

In order to measure the influence of chip formation or chip separation on the internal strain state of the workpiece, it was originally intended to provide the trigger point with a slight time offset from cut to cut in this very dynamic milling process. Each individual measurement would thus take place at a different cutting depth and a slightly different rotation angle of the tool. Provided that the workpiece is homogeneous and the tool encounters the same initial state of the workpiece at each cut, the chip removal and its influence on the strain state of the workpiece could then be investigated with an extremely high time resolution. The smallest resolution (smallest meaningful trigger time offset) is defined by the jitter of the laser pulses, which amounts to 5 µs. At a cutting speed of $v_c = 7.7 \frac{m}{s}$, the trigger point could be shifted by this smallest unit to allow measurements of tool shifts of approx. 40 µm on the circular path.

The results from Figure 11 in Section 3.3 illustrate why this approach does not work. In a subsequent cut, the tool never encounters the initial state of the workpiece, but rather a mechanically excited system with an inhomogeneous strain or residual stress state. In the periodic milling process

shown, 60 ms elapse between tool intervention and the next intervention. The time required for the workpiece to reach a stable final state after excitation, however, is approx. 300 ms. Especially in the case of multiple loads with periodically recurring stresses, which occur more frequently than every 300 ms, it can be assumed that the process encounters an excited workpiece and that the previous load must therefore also be taken into account.

After a sufficient decay time, the measured modifications finally are one order of magnitude below the measured maximum loads.

The chip formation and the chip breakage were theoretically investigated by means of a FEM simulation. It could be shown that strain waves propagate through the workpiece at approx. $3320 \pm 452 \frac{m}{s}$, which are released from the workpiece side due to the tool exit. The propagation velocity of the simulated strain front corresponds within the uncertainty of the propagation velocity to the literature values for a sound wave in structural steel.

Furthermore, it is to be expected that the propagating strain front is reflected at the boundary surfaces and therefore passes through the workpiece several times before the wave vanishes due to the damping of the material.

This leads to the question, when do the oscillations excited by the impact theoretically come to a rest? According to Roderick and Truell [16], the sound absorption coefficient for steel alloy (50CrMo4) is approx. 60 dB/1000 m at a sound frequency of less than 2 MHz. The sound wave with a propagation velocity of $3320 \frac{m}{s}$ would require approximately 300 ms for the distance of 1000 m. According to the measurement results from Figure 11, the remaining modification change after 300 ms has actually dropped to about one thousandth of the maximum (60 dB). Therefore, for low frequencies of the excitation pulse due to the tool intervention, the measured excitation duration basically corresponds to the literature values.

The formation of chatter marks (see Figure 1) is explained in current research reports by chip formation and chip breakage, which stimulate the entire tool system and the workpiece to vibrate. The aspect that the tool encounters a workpiece that is usually excited periodically and in which the cutting forces and the dynamic strains already introduced are superimposed has not yet been considered. The results of this article show that although the dynamic excitation is smaller by a factor of 10 than the maximum occurring loads, these material dynamics should nevertheless be included in the research of chip removal. It is very probable that the current strain state influences the chip formation and in particular chip breakage. Therefore, it cannot be ruled out that the investigated dynamic expansion waves or shock waves, with their change in the residual stress state of the workpiece, have an influence on the formation of chatter marks.

Therefore, when investigating process dynamics, such as the formation of chatter marks, not only the vibration and resonance behavior of the machine tool or the workpiece should be considered in the future, but also the internal dynamic strain condition of the workpiece at the time the tool is engaged.

In order to display the dynamic deformation processes in the future with sufficient temporal resolution and also to be able to observe such things as chip breakage or the formation of chatter marks, at least three measurements should be taken in a minimum measuring field of 10 mm. At a sound velocity of $3330 \frac{m}{s}$ an image acquisition rate of one million frames per second is required. A currently purchased camera system (Photron FASTCAM NOVA S12, Photron USA, Inc., San Diego, USA, 2019) is capable of this measurement frequency. Upcoming measurements during the single-tooth circumference milling process will be carried out with this system.

At the same time, it should be examined furthermore whether the measurement uncertainty and the resolution behavior of the system are sufficient to be able to make predictions about the residual stress states of the workpiece based on the determinations of the sound velocity components.

5. Conclusions

In machining processes such as single-tooth milling, dynamic vibrations of the manufacturing system usually occur. In contrast to these well-known effects, this paper examines the question of

whether additional mechanically-induced dynamic loads in the workpiece are stimulated by the tool impact. For this purpose, the load during tool engagement is first measured by means of speckle photography and its applicability for in-process use is confirmed by comparison with theoretical predictions. Subsequently, it is shown both metrologically and simulatively that the tool impact induces "shock waves" during milling in the form of deformations and strains which propagate through the workpiece at the speed of sound. In the present case, the wave ebbs after many multiple reflections at the boundary surfaces, so that the resulting dynamic excitation decays after 300 ms. The cyclic multiple loads have a period duration of 60 ms, which is shorter than the sound decay time. Therefore, it can be assumed that the tool encounters an already excited initial state during machining. Especially in the description of chip formation, chip breakage, and the formation of chatter marks, the material-internal dynamic strain variations should therefore also be considered. Overall, the results illustrate the potential of speckle photography in combination with modern high-speed cameras and compact short-pulse lasers. Speckle photographic in-process measurements of dynamic deformations and strains can provide deeper insights into individual manufacturing processes. This enables the optimization of manufacturing processes (e.g., by specifically adapting the resonance behavior via the design of the workpiece geometry or the clamping device).

Author Contributions: Conceptualization, A.T. and D.S.; methodology, A.T. and D.S.; project administration, A.F.; supervision, A.F.; validation, A.T.; writing—original draft, A.T.; writing—review and editing, D.S. and A.F.

Acknowledgments: The authors gratefully acknowledge the financial support by the German Research Foundation (DFG) for subproject C06 “Surface optical measurement of mechanical working material loads” within the Transregional Cooperative Research Center SFB/TRR136. They also thank Melanie Willert (subproject F05) and their colleagues from the Laboratory for Micro Manufacturing for the friendly support during the conduction of the in-process measurements.

Conflicts of Interest: The authors declare no conflicts of interest.

References

1. Brinksmeier, E.; Klocke, F.; Lucca, D.A.; Sölter, J.; Meyer, D. Process Signatures—A New Approach to Solve the Inverse Surface Integrity Problem in Machining Processes. *Procedia CIRP* **2014**, *13*, 429–434. [CrossRef]
2. Brinksmeier, E.; Gläbe, R.; Klocke, F.; Lucca, D.A. Process Signatures—An Alternative Approach to Predicting Functional Workpiece Properties. *Procedia Eng.* **2011**, *19*, 44–52. [CrossRef]
3. Tausendfreund, A.; Stöbener, D.; Dumstorff, G.; Sarma, M.; Heinzel, C.; Lang, W.; Goch, G. Systems for locally resolved measurements of physical loads in manufacturing processes. *CIRP Ann. Manuf. Technol.* **2015**, *64*, 495–498. [CrossRef]
4. Tausendfreund, A.; Borchers, F.; Kohls, E.; Kuschel, S.; Stöbener, D.; Heinzel, C.; Fischer, A. Investigations on material loads during grinding by speckle photography. *J. Manuf. Mater. Process.* **2018**, *71*, 12. [CrossRef]
5. Archold, E.; Burch, J.M.; Ennos, A.E. Recording of in-plane surface displacements by double-exposure speckle photography. *Opt. Acta* **1970**, *17*, 883–898. [CrossRef]
6. Stetson, K.A. A Review of Speckle Photography and Interferometry. *Opt. Eng.* **1975**, *14*, 482–489. [CrossRef]
7. Fischer, A. Fundamental uncertainty limit for speckle displacement measurements. *Appl. Opt.* **2017**, *56*, 7013–7019. [CrossRef] [PubMed]
8. Tausendfreund, A.; Stöbener, D.; Fischer, A. Precise in-process strain measurements for the investigation of surface modification mechanisms. *J. Manuf. Mater. Process.* **2018**, *2*, 9. [CrossRef]
9. Weck, M.; Brecher, C. *Werkzeugmaschinen, Fertigungssysteme: Messtechnische Untersuchung und Beurteilung, dynamische Stabilität*; VDI-Buch; Springer: Heidelberg, Germany, 2006.
10. Kalveram, M. *Analyse und Vorhersage der Prozessdynamik und der Prozessstabilität beim Hochgeschwindigkeitsfräsen*; Dissertation Universität Dortmund, Vulkan Verlag Essen: Essen, Germany, 2005.
11. Buchkremer, S.; Klocke, F.; Veselovac, D. 3D FEM simulation of chip breakage in metal cutting. *Int. J. Adv. Manuf. Technol.* **2016**, *82*, 645–661. [CrossRef]
12. Zhou, P.; Goodson, K.E. Subpixel displacement and deformation gradient measurement using digital image/speckle correlation (DISC). *Opt. Eng.* **2001**, *40*, 1613–1620. [CrossRef]

13. Kajberg, J.; Lindkvist, G. Characterisation of materials subjected to large strains by inverse modelling based on in-plane displacement fields. *Int. J. Solids Struct.* **2004**, *41*, 3439–3459. [CrossRef]
14. Wang, Z.; Rahman, M. High-Speed Machining. *Compr. Mater. Process.* **2014**, *11*, 221–253.
15. Rose, J.L. *Ultrasonic Waves in Solid Media*; Cambridge University Press: Cambridge, UK, 2004.
16. Roderick, R.L.; Truell, R. The Measurement of Ultrasonic Attenuation in Solids by the Pulse Technique and Some Results in Steel. *J. Appl. Phys.* **1951**, *23*, 267–279. [CrossRef]